Added Resistance Simulation of Blunt Ship in Short Wave

by Jikang Chen[*] and Wenyang Duan
College of Shipbuilding Engineering, Harbin Engineering University, Harbin, China
E-mail: *cjkhrb@sina.com*

Highlights:
- Added resistances of KVLCC2 in short waves are predicted by 2nd order TEBEM and compared with published results by other numerical solutions and experimental results.
- It is found the strength of low-pass filter in numerical treating the free surface elevation plays an important role for accurate predicting the added resistance in short wave.

1. Introduction

The rankine panel method (RPM) for wave-ship interaction has been widely used nowadays. The advantage of RPM is possibility to deal with more complicated free-surface conditions. Nakos (1990), Kring (1994) and Huang (1997) analysed the nonlinear ship motion by a time-domain three dimensional RPM. Kim et al. (2011) compiled a seakeeping analysis program (WISH) for the linear and nonlinear seakeeping analysis and wave loads forecasting by the B-spline RPM. Shao and Faltinsen (2012) proposed a body-fixed formulation to avoid the difficulty which needs to calculate the high order derivatives in the earth coordinate system by HOBEM.

However, a disadvantage of the Rankine panel methods is the necessity of discretization of the free surface surrounding the body, which increases the number of unknowns and also introduces the numerical instability due to the saw-tooth behavior in the time domain numericalsimulations for forward speed problems. Vada and Nakos (1993) and Kim et al (1997) considered that the instability observed in their numerical simulation process were caused by the energy from the external force, which would be accumulated on a wave period with zero group velocity. Buchmann (2000b) pointed out the non-uniformity in the spatially discretized models may cause this phenomenon. However, the reason for the instability has not been fully understood. Several researchers utilized the low-pass filter to suppress the numerical instability. Nakos (1990) and Kring (1994) used five-point filter formulation to suppress the spurious waves for the ship motion RAOs. The seven-point formulation is used by Kim (1997) for the nonlinear interactions of surface waves with bodies without forward speed. He and Kashiwagi (2012) studied the ship steady wave problem using the seven-point formulation. Shao and Faltinsen (2012) utilized a three-point filter to retrain the saw-tooth behavior for the added resistance problem for the fine ship. These numerical experiments had not shown the impacts of the filter for the simulation of blunt ship added resistance problems.

The ship motions are negligible in short waves, and the added resistance is mainly due to wave reflection at the bow. Because the reflection added resistance is very small for fine ship, the strength or frequency of application of the filter causes almost no influence on added resistance of fine ship. However, for large blunt ship, the reflection added resistance in short wave give important contribution in low sea state. It is found application of low-pass filter has sensible influence on the numerical results of added resistance of blunt ship. The strength and frequency of using filter is discussed for KVLCC2 ship.

2. Numerical Method

For forward speed ship motion problems, the velocity potential consists of three components: the steady potential Φ which is computed based on the double-body flow, incident wave potential φ_I and disturbing wave potential φ_d respectively. The potential Φ and φ_d can be obtained by solving each of the following problems :

$$
\begin{cases}
\nabla^2 \Phi = 0 \\
\dfrac{\partial \Phi}{\partial n} = \vec{U} \cdot \vec{n} \quad (on\ S_H) \\
\dfrac{\partial \Phi}{\partial z} = 0 \quad\quad (on\ S_F) \\
\Phi = 0 \left(\sqrt{x^2 + y^2 + z^2} \to \infty \right)
\end{cases}
\tag{1a}
$$

$$
\begin{cases}
\nabla^2 \varphi_d = 0 \\
\left[\dfrac{\partial}{\partial t} - \left(\vec{U} - \nabla \Phi\right) \cdot \nabla \right] \zeta_d = \zeta_d \dfrac{\partial^2 \Phi}{\partial z^2} + \dfrac{\partial \varphi_d}{\partial z} \quad\quad (on\ S_F) \\
\left[\dfrac{\partial}{\partial t} - \left(\vec{U} - \nabla \Phi\right) \cdot \nabla \right] \varphi_d = \vec{U} \cdot \nabla \Phi - g\zeta_d - \dfrac{1}{2}\left(\nabla \Phi\right)^2 \quad (on\ S_F) \\
\dfrac{\partial \varphi_d}{\partial n} = \sum_{j=1}^{6} \left(\dfrac{\partial \xi_j}{\partial t} n_j + \xi_j m_j \right) - \dfrac{\partial \varphi_I}{\partial n} \quad\quad (on\ S_H) \\
\varphi_d \big|_{t=0} = 0,\ \dfrac{\partial \varphi_d}{\partial n}\big|_{t=0} = 0 \quad\quad (initial\ condition)
\end{cases}
\tag{1b}
$$

Where $\vec{U}$ is the ship forward speed, ξ_j means the displacement in *j* direction, $\vec{n}$ is the normal vector points out of the fluid domain. The added resistance is calculated by the near-field formulation.

$$\vec{F}_2 = \int_{WL} \frac{1}{2}\rho g \left[\zeta - (\xi_3 + \xi_4 y - \xi_5 x) \right]^2 \cdot \vec{n} dL - \rho \int_{WL} \left[-\left(\vec{U} - \frac{1}{2}\nabla \Phi \right) \cdot \nabla \Phi \right] \left[\zeta - (\xi_3 + \xi_4 y - \xi_5 x) \right] \cdot \vec{n}_1 dL$$

$$- \rho \int_{WL} \vec{\delta} \cdot \nabla \left[-\left(\vec{U} - \frac{1}{2}\nabla \Phi \right) \cdot \nabla \Phi \right] \left[\zeta - (\xi_3 + \xi_4 y - \xi_5 x) \right] \cdot \vec{n} dL - \rho \iint_{S_H} gz\, \vec{n}_2 ds$$

$$- \rho \iint_{S_H} \frac{1}{2}\nabla(\varphi_I + \varphi_d)^2 \cdot \vec{n} ds - \rho \iint_{S_H} \vec{\delta} \cdot \nabla \left[\frac{\partial(\varphi_I + \varphi_d)}{\partial t} - (\vec{U} - \nabla \Phi) \cdot \nabla(\varphi_I + \varphi_d) \right] \cdot \vec{n} ds \qquad (2)$$

$$- \rho \iint_{S_H} \left[g(\xi_3 + \xi_4 y - \xi_5 x) + \frac{\partial(\varphi_I + \varphi_d)}{\partial t} - (\vec{U} - \nabla \Phi) \cdot \nabla(\varphi_I + \varphi_d) \right] \cdot \vec{n}_1 ds$$

$$- \rho \iint_{S_H} \left[-\left(\vec{U} - \frac{1}{2}\nabla \Phi \right) \cdot \nabla \Phi \right] \cdot \vec{n}_2 ds - \rho \iint_{S_H} \vec{\delta} \cdot \nabla \left[-\left(\vec{U} - \frac{1}{2}\nabla \Phi \right) \cdot \nabla \Phi \right] \cdot \vec{n}_1 ds$$

Where ζ is the wave elevation, δ is the total displacement of ship motion, *WL* represents the waterline.

TEBEM method (Duan et al. ,2014) is used to solve the boundary value problem. A low-pass filter similar(Shao and Faltinsen, 2012) is applied on the collocation points on the free surface to restrain the instability of wave elevation.

$$\bar{\zeta}_j = c\zeta_{j-1} + (1 - 2c)\zeta_j + c\zeta_{j+1} \qquad (3)$$

Where the subscript j is mesh number of collocation point. c is the strength of low-pass filter, $\bar{\zeta}$ means the wave elevation after smoothing. The filter will affect the solution of velocity potential indirectly through the dynamic free-surface conditions. At each time step the filter is first applied in the azimuthal direction for all points on the free surface panels and then the filter is used in the radial direction for all points on the free surface.

3. Numerical Results and Discussion

To show the role of the strength of low-pass filter on the added resistance in short wave, A typical public blunt ship KVLCC2 ship model in head sea is selected as demonstration.

Calculation condition for KVLCC2 in short wave

Ship motion	Heave and Pitch	Wave length λ / L	0.3
Time-step	0.01T	Simulation time	35T
Free-surface panel	1525	Free-surface size	$5L_{PP}$
Body-surface panel	1212	Damping zone type	O-type grid
Strength of the filter	0.002,0.003,0.004	Damping zone size	$2L_{PP}$
Forward speed	Fr=0.142	Damping zone strength	$\mu_0 = 15$

Figure 1 and 2 show the panel discretization on the half free surface and body surface, the triangle elements were used on hull surface of the bow and stern part. Fig.3 and 4 show the motion response of the heave and pitch of KVLCC2 model respectively, where the length ratio of wave to ship is from 0.3 to 2.0. The added resistance is shown in Fig.5. The agreement is good between the 2nd TEBEM and the other numerical solution and experiment results. In Fig.6, the contribution of the bow, stern and middle part of KVLCC2 for added resistance at $\lambda / L = 0.3$ is shown. It is found the contribution to the added resistance in short waves is primarily from bow segment, whereas the stern and middle part is quite small. Fig.7 and 8 show the contribution from the waterline and square of velocity integration for the added resistance at the bow part. It can be seen the waterline integration is almost twice of the square of velocity integration but in opposite sign.
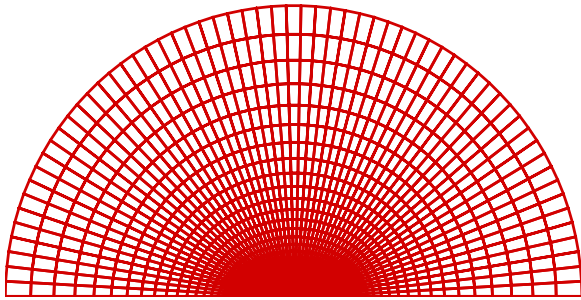
Fig.1 the panel sketch of the free surface
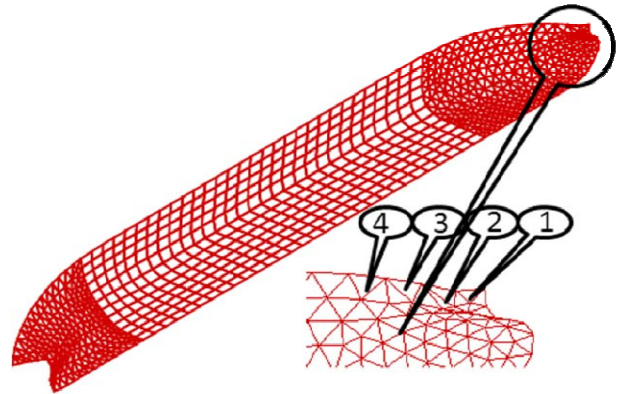
Fig.2 the panel sketch of the body surface
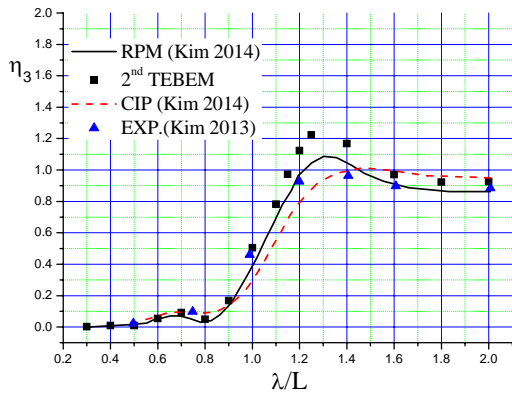
Fig.3 comparison of heave RAOs between experiment and numerical solution
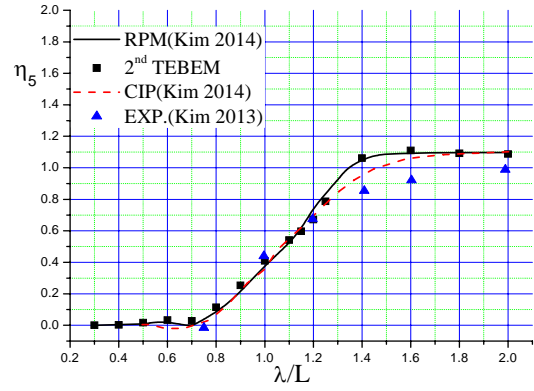
Fig.4 comparison of pitch RAOs between experiment and numerical solution
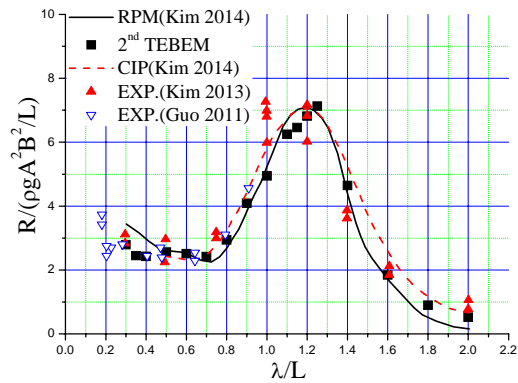
Fig.5 comparison of added resistance between experiment and numerical solution
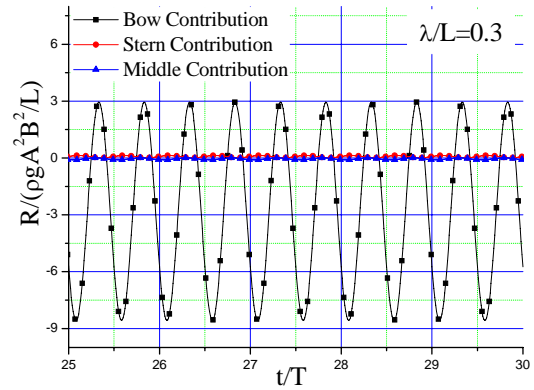
Fig.6 added resistance components from the different parts of the KVLCC2 at $\lambda / L = 0.3$
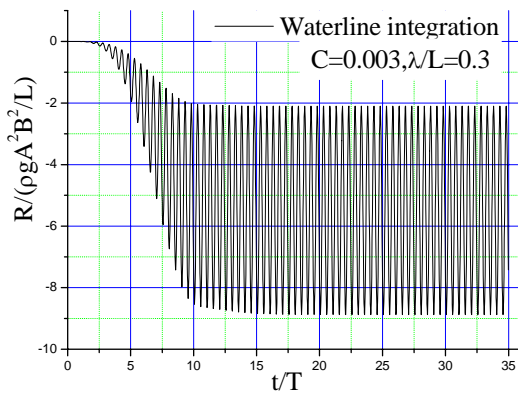
Fig.7 contribution of the waterline integration for added resistance due to the bow part at $\lambda / L = 0.3$
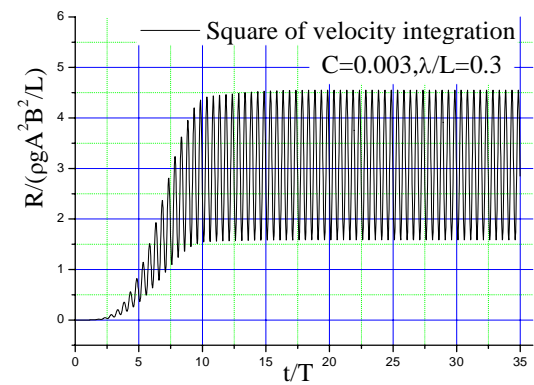
Fig.8 contribution of the square of velocity integration for added resistance due to the bow part at $\lambda / L = 0.3$
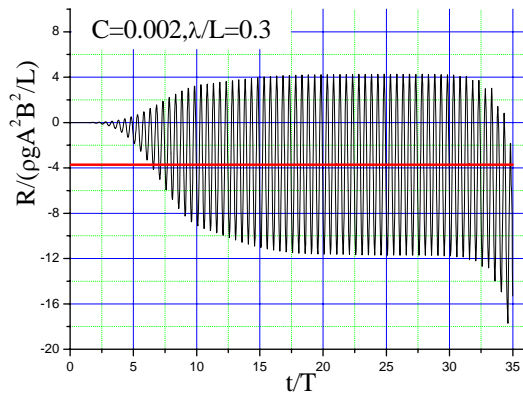
Fig.9 the history of added resistance at $\lambda / L = 0.3, C = 0.002$
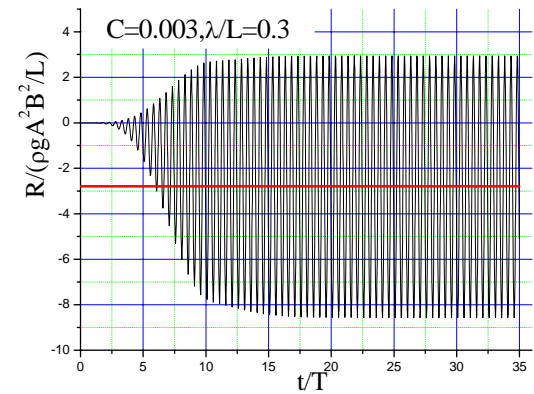
Fig.10 the history of added resistance at $\lambda / L = 0.3, C = 0.003$
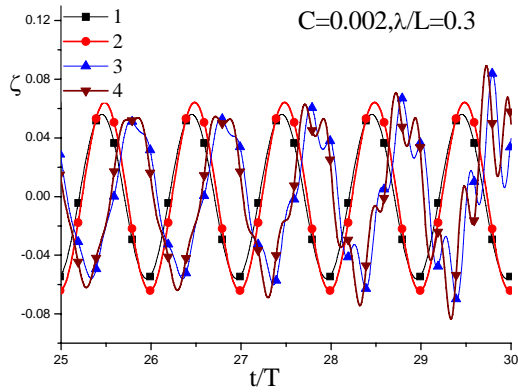
Fig.11 the history of wave elevation at waterline collocation points at $\lambda / L = 0.3, C = 0.002$
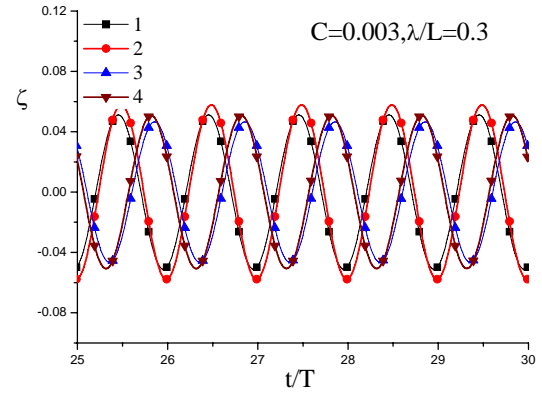
Fig.12 the history of wave elevation at waterline collocation points at $\lambda / L = 0.3, C = 0.003$
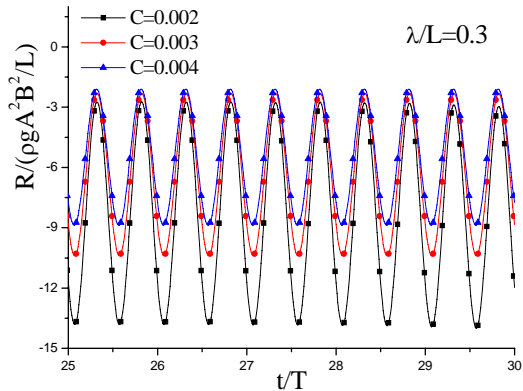
Fig.13 the history of added resistance due to the waterline integration on the bow part surface at $\lambda / L = 0.3$
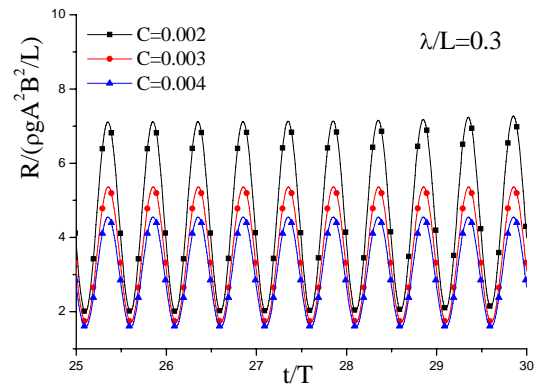
Fig.14 the history of added resistance due to the square of velocity integration on the bow part surface at $\lambda / L = 0.3$

Fig.9 and 10 show the history of the added resistance value with different strength of low-pass filter, the wave elevation around the bow are shown in Fig.11 and 12. It can be seen the history is not stable when the strength of filter is equal to 0.002. Form Fig. 9 and 11, although the added resistance is stable for period $t / T = 20 - 30$, but it is changed after 30 and the wave elevation values has been chaotic for period $t / T = 20 - 30$. So the added resistance is not consistent with local fluid flow as $C = 0.002$. Fig.13 and 14 show the waterline and square of velocity integration vary with different strength of filter, it can be concluded that the strength of filter play a key role for the added resistance prediction in short waves.

References

[1] Nakos D.E., 1990, Ship Wave Patterns and Motions by a Three Dimensional Rankine Panel Method. PhD. Thesis, MIT.

[2] Kring D.C., 1994, Time domain ship motions by a three dimensional Rankine panel method, PhD. Thesis, MIT.

[3] Huang Y.F., 1997, Nonlinear ship motions by a Rankine panel method, PhD. Thesis, MIT.

[4] Song M.J., Kim K.H. and Kim Y.H., 2011, Numerical analysis and validation of weakly nonlinear ship motions and structural loads on a modern containership, Ocean Engineering, 38,77-87.

[5] Shao Y.L and Faltinsen O.M., 2012, Linear seakeeping and added resistance analysis by means of body-fixed coordinate system, J. Mar. Sci. Technol., 17(4), 493-510.

[6] Vada T. and Nakos D., 1993, Time-marching schemes for ship motion simulations. 8th International Workshop on Water Waves and Floating Bodies, Canada (Newfoundland).

[7] Kim Y.H., Kring D.C. and Sclavounos P.D., 1997, Linear and nonlinear interactions of surface waves with bodies by a three dimensional Rankine panel method. Applied Ocean Research, 19, 235-249.

[8] Buchmann B., 2000b, Accuracy and stability of a set of free-surface time-domain boundary element models based on B-splines. Int. J. Numer. Methods Fluids. 33(1), 125-155.

[9] He G.H. and Kashiwagi M., 2012, Time Domain Simulation of Steady Ship Wave Problem by a Higher-Order Boundary Element Method. Proceedings of 22th International Offshore and Polar Engineering Conference. Greese.

[10] Duan W.Y., Chen J.K. and Zhao B.B., 2014, Second order wave loads based on second order TEBEM, 29th International Workshop on Water Waves and Floating Bodies, Japan(Osaka).

[11] Guo B.J. and Stern S., 2011, Evaluation of added resistance of KVLCC2 in short waves. Journal of Hydrodynamics, 23(6), 709-722.

[12] Kim K.H., Yang K.K. and Seo M.G., 2013, Computational analysis of added resistance in short waves, International Research Exchange Meeting of Ship and Ocean Engineering in Osaka.